Molecular Dynamics Study of the Rate of Melting of a Crystalline Polyethylene Molecule: Effect of Chain Folding

Bobby G. Sumpter,*,†,‡ Donald W. Noid,*,†,‡ Bernhard Wunderlich,*,†,‡ and Stephen Z. D. Cheng*,§

Chemistry Division, Oak Ridge National Laboratory, Oak Ridge, Tennessee 37831-6182, Department of Chemistry, The University of Tennessee, Knoxville, Tennessee 37996-1600, and Institute and Department of Polymer Science, The University of Akron, Akron, Ohio 44325-0604

Received November 3, 1989; Revised Manuscript Received April 12, 1990

ABSTRACT: Molecular dynamics is used to study the melting on the surface of a polyethylene-like crystal. The rate constant for melting of a crystalline molecule without and with one to four folds is determined at several different temperatures and molecular lengths. The results show a strong dependence of the transition rate on the number of folds. For a constant lamellar thickness, the transition rate decreases with increasing number of folds for temperatures near the equilibrium melting temperature, as expected from analogy with experimental melting temperatures. In contrast, the transition rate increases with increasing number of folds for temperatures that exceed the equilibrium melting temperature by more than 100 K. Two melting paths are suggested to explain the simulation data. One pathway involves a competition between melting and crystallization. This pathway leads to a decreasing transition rate as a function of increasing folding. The second pathway exhibits dominating melting. In this case, the rate of transition tends to increase with increasing number of folds. Diffusion coefficients of segments at different locations along the chain show that motion of the ends of a polymer chain or of the folds is faster than in the center of the stem. The overall effect of increasing temperature is to increase the diffusion coefficients.

I. Introduction

Two-dimensional polymer crystal melting on an extended-chain crystal surface was studied experimentally some years ago. Recrystallization of the melt on the extended-chain surface does not lead to any re-extended-chain crystals, but rather to folded-chain crystals decorating the underlying extended-chain crystal surface.[1-3] From the viewpoint of equilibrium statistical mechanics, melting occurs from an extended-chain crystalline state to a liquid phase. In the crystalline state, the internal degrees of freedom are well ordered, while in the fluid phase there is a large amount of disorder. For polyethylene, the extended-chain crystalline state consists of all-trans conformations. As the temperature is increased toward the melting point, there is a critical temperature well below the melting point at which there can be conformational disorder.[4] However, this disorder, which results from large-angle rotations about the C–C bonds, including and beyond the gauche conformation, does not lead to any coiling of the chain. There is still order along the crystal axes. This type of mesophase has been called a condis crystal.[5] In the liquid phase, finally, there is a mixture of gauche and trans rotations that lead to a randomly coiled chain with disorder about all axes.

Quantitative studies of polymer melting rates were made for polyethylene,[2,3] selenium,[6,7] and poly(ethylene oxide).[8,9] Two different types of melting have been observed. One shows a linear relationship between the melting rate and superheating ΔT, and the other, a linear relationship between the logarithmic melting rate and ΔT,[10] where $\Delta T = T - T_m^\circ$. The constant T_m° represents the equilibrium melting temperature of the particular polymer studied. The question of "continuous" or "nucleation-controlled" mechanisms is applicable to these observations. The former melting process is continuous, while the latter is obviously of a different nature and is most likely nucleation controlled. The nucleation barrier (ΔG) is usually small enough so that significant melting starts close to T_m°. On the other hand, the reverse process (crystallization) occurs only below a certain supercooling. In this temperature range of supercooling a metastable, supercooled melt exits.

Crystallization/melting for small molecules is thermodynamically a first-order transition, but for macromolecules this process is complicated by nonequilibrium processes. In contrast to the crystal-to-melt transition, the melt-to-crystal transition involves significant kinetic effects. We have suggested that molecular nucleation and not secondary nucleation may be the rate-determining step in crystallization.[3,11-15] This suggestion is based on experimental observations and has recently been studied by computer simulations.[16]

While the melting transition described by a universal statistical mechanical theory[17] has been considered in depth,[18] the atomistic details of the process are required for a complete understanding. There is a need for more reliable and rigorous calculations for simple models in order to develop a better understanding of polymer melting/crystallization. In this light, we have recently carried out molecular dynamics simulations of the melting process in linear macromolecules.[10] In that study, a simplified molecular model was used to obtain information on one molecule. The results showed that the end-to-end distance and radius of gyration have during melting a simple exponential dependence on time. Melting rate constants were determined for various temperatures and molecular lengths. The melting rate was found to increase with increasing temperature and decrease with increasing molecular length. In the present paper, we extend our first study to include polymer chain folding. The effect of the number of folds on the rate of the transition will be studied, as well as the temperature and molecular length dependence. A detailed analysis of the time-dependent structural changes (extended chain to random coil) is presented. In section II, we describe the model and methods that we have used to study the dynamics of the melting process. The results are presented in section III, and the conclusions

† Oak Ridge National Laboratory.
‡ The University of Tennessee.
§ The University of Akron.

0024-9297/90/2223-4671$02.50/0

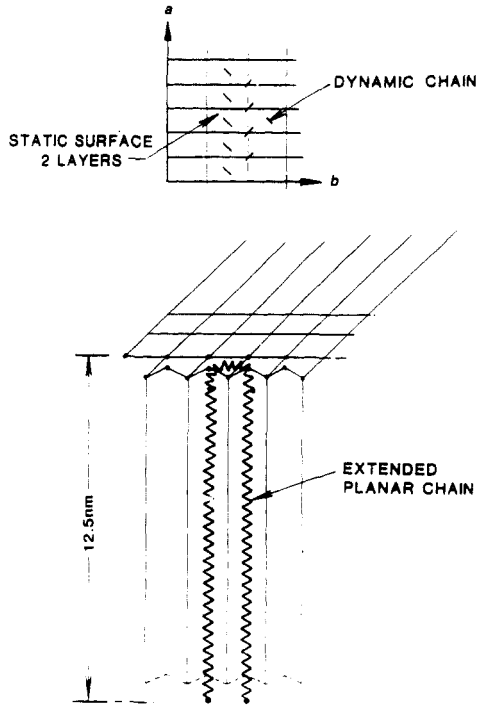

Figure 1. Plot of the orthorhombic crystal lattice with two dynamic and nine surface layer chains. The bottom graph shows the connection of the two chains by a fold.

are given in section IV.

II. Method

A. Model. Our model for a polyethylene (PE) crystal surface consists of two layers of static chains arranged in an extended zigzag on lattice sites of the orthorhombic phase of PE with the crystal dimensions a = 0.495 nm, b = 0.7 nm, and c = 0.255 nm (Figure 1). As part of the crystal, one chain with n atoms and m folds lies on the crystal surface at an appropriate lattice site (see Figure 1). Such a chain provides a new interface layer between the crystal and melt. The total surface area of the crystal, however, does not change by addition of such a chain. The molecular dynamics method gives the momenta and coordinates of each atom in the system as a function of time by integration of first-order differential equations known as Hamilton's equations of motion. For the set of atoms of interest arranged into polymer chains, Hamilton's equations (a variation of Newton's equation)[19] are

$$H = \sum_{i=1}^{N} \frac{1}{2m_i}(p_{x_i}^2 + p_{y_i}^2 + p_{z_i}^2) + \sum_{i=1}^{N-1} v_2(r_i) + \sum_{i=1}^{N-2} V_3(\theta_{i;i+1;i+2}) + \sum_{i=1}^{N-3} V_4(\tau_{i;i+1;i+2;i+3}) + \sum V_{2\mathrm{NBC}}(r_{ij}) + \sum V_{2\mathrm{NBS}}(r_{ij}) \quad (1)$$

$$\dot{q}_i = \frac{\partial H}{\partial p_{q_i}} = \frac{p_{q_i}}{m_i} \quad (2)$$

and

$$\dot{p}_i = -\frac{\partial H}{\partial q_i} = -\frac{\partial V}{\partial q_i} \quad (3)$$

where H is the Hamiltonian and is composed of kinetic energy terms (first term in eq 1) and potential energy terms (remaining terms in eq 1), N is the number of atoms in a chain, q_i is the Cartesian coordinate (either x, y, or z) of the ith atom, p_{q_i} is the corresponding momentum (in either the x, y, or z direction) of the ith atom, and the subscripted V's are the individual terms of the potential energy to be discussed shortly. The r_{ij}, θ_{ijk}, and τ_{ijkl} are the internal coordinates for the interatomic distance, the angle between three consecutive atoms, and the torsional (twist) angle between four consecutive atoms, respectively (see Figure 2). The Hamiltonian represents the kinetic energy part in Cartesian momenta. In our calculations, we have collapsed the CH_2 repeating group to a single particle of mass 14.5 amu. The potential energy functions are written in terms of two-body, three-body, and four-body bonded interactions (i.e., V_2, V_3, and V_4) and an additional, nonbonded two-body term labeled $V_{2\mathrm{NBC}}$ or $V_{2\mathrm{NBS}}$. We have used two different nonbonded interactions. On ($V_{2\mathrm{NBC}}$) is to describe the interactions of the atoms 1 to N within the polymer chain, and the second ($V_{2\mathrm{NBS}}$) describes the interactions of the atoms of the chain with the crystal surface.

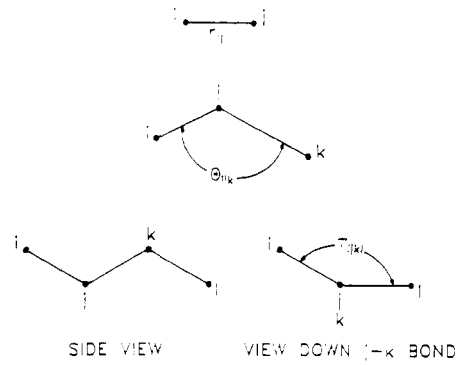

Figure 2. Definition of the internal coordinates.

Table I
Potential Energy Parameters

two-body constants[a]	
K_r	2.65098×10^5 kJ/mol nm^2
r_e	0.153 nm
three-body constants[a,b]	
K_θ	130.122 kJ/mol
cos θ = cos 113°	0.3907
$K_{\theta A}$	331.37 kJ/mol·rad kcal/mol·rad^2
θ_{0A}	113°
four-body constants[b]	
α	−18.41 kJ/mol
β	26.78 kJ/mol
two-body nonbonded constants[b]	
PE chain interactions	
ϵ	0.4137 kJ/mol
σ	0.4335 nm
chain–surface interactions[c]	
ϵ	0.3072 kJ/mol
σ	0.4335 nm

[a] Waber, T. A. *J. Chem. Phys.* **1978**, *69*, 2347; **1979**, *70*, 4277. [b] Sorensen, R. A.; Liam, W. B.; Boyd, R. H. *Macromolecules* **1988**, *21*, 1941. Boyd, R. H. *J. Chem. Phys.* **1968**, *79*, 2574. [c] Fit to give the heat of fusion of polyethylene.

The two-body potential is a harmonic oscillator of the form

$$V_2(r) = \frac{K_r}{2}(r_{ij} - r_e)^2 \quad (4)$$

where r_{ij} is the intermolecular distance between atoms i and j, and K_r and r_e are constants given in Table I.

The three-body term is

$$V_3(\theta) = 1/2K_\theta(\cos\theta - \cos\theta_0)^2 \quad (5)$$

θ is the angle between atoms i, j, and K (see Figure 2). In order to study the effect of bond-bending flexibility on the melting transition, we have also considered an alternate

three-body potential

$$V_{3A}(\theta) = 1/2K_{\theta A}(\theta - \theta_{0A})^2 \quad (6)$$

The four-body potential is

$$V_4(\tau) = 8.77 + \alpha \cos \tau + \beta \cos^3 \tau \quad (7a)$$

or

$$V_4(\tau) = 0 \quad (7b)$$

The nonbonded interactions are of the form

$$V_{NB}(R) = 4\epsilon[(\sigma/R)^{12} - (\sigma/R)^6] \quad (8)$$

All constants in the potential energy terms are given in Table I.

Hamilton's equations (eqs 2 and 3) were integrated in Cartesian coordinates using the differential equation solver ODE[20] and a new method developed in this laboratory for evaluation of the internal derivatives in eq 3.[21]

It is important to note that our molecular dynamics simulations[21] involve very accurate numerical integrations of Hamilton's equations of motion. Calculations are carried out in the *microcanonical ensemble* (total energy is constant), and conservation of the total energy to at least four numerical digits is required by our integrations. This degree of accuracy is necessary to study the details of structure and dynamics of polymers in which we are interested.

In our present model, we have an environment that describes a PE crystal in a vacuum. That is, the dynamic PE chain has no forces above the surface. While at a constant temperature this would mean that the PE chain would collapse into a droplet upon melting, due to our simulations which are carried out in the microcanonical ensemble, the PE chain approaches a random coil structure and not a droplet. In future calculations we will study the effects of a constant-temperature environment by using Nosé or Langevin[22] equations and also include a mean field to simulate a liquid environment which gives the PE chain a well-defined state for the transition upon melting (instead of a vacuum).

B. Trajectories. Initially, a randomly chosen amount of kinetic energy is placed in each atom of the dynamic chain. The end-to-end distance (EED) and radius of gyration (R_g) are then calculated as a function of time. If the time of computer simulation is long enough, the values of EED and R_g will reach a constant value. Rate constants for melting are determined by computing the least-squares fit of the slope of ln $R_g(t)$ vs time (t). The data for ln $R_g(t)$ vs t are fitted over the range 0–100 ps. An analysis of the data is performed such that the rate constants are essentially converged. That is, rate constants are calculated for the first 10 ps of the data and then 20, 30, ..., 100 ps to determine the converged value. Rate constants for crystallization can be calculated by a similar procedure. The rate of crystallization is the slope of ln (number of atoms reoriented) vs time.

Diffusion coefficients for different segments in the PE chain were computed with the velocity autocorrelation function and the relation

$$D = 1/3 \int_0^\infty \langle \mathbf{V}_{CM}(0)\mathbf{V}_{CM}(t) \rangle \, dt \quad (9)$$

The segment center-of-mass velocity is given by

$$\mathbf{V}_{CM} = \sum_{i=N_{in}}^{N_{out}} \mathbf{p}_i / \sum_{i=N_{in}}^{N_{out}} M_i \quad (10)$$

where $\mathbf{p}_i$ is the Cartesian momentum of atom i and M_i is the mass. The sum is over various segments of the chain, starting from atom N_{in} and ending with atom N_{out}.

The Cartesian coordinates of the folded chains were generated by the following procedure:

(1) The Cartesian coordinates of a single chain of PE are generated which give the correct bond lengths, bond angles, and dihedral angles using the program EUCLID.[22] This chain is translated by one lattice site on the crystal, thus giving two N-atoms chains on the PE crystal.

(2) An M-atom fold is added to connect the two chains.

(3) The equations of motion are integrated (eqs 1–3), and the $2N + M$ atoms are annealed (setting the momenta to zero) until the fold has found a potential minimum (the kinetic energy is zero). The coordinates are then saved and used as the initial geometry of once-folded ($2N + M$)-atom PE chain.

III. Results

A. Melting/Crystallization. We have carried out molecular dynamics simulations of both extended and multiply folded chains. Up to 1000 dynamic CH_2 groups have been included in our simulation. The effects of bending and torsional modes on the extended to random coil transition, "melting", have been studied by changing the form of the potential (eqs 5–7).

Figure 3A is a time sequence of melting at high temperature of the molecular configuration of a single, 100-atom extended chain of polyethylene. The time frames are taken at the intervals listed in the legend. This figure shows how an extended polymer chain coils up on the underlying, static crystal surface. As can be seen by examining Figure 3A, the initial step to this process is the movement (peeling off) of the ends of the chains. At a sufficiently longer time, the middle of the chain begins to move also. The diffusion of the middle of the chain is followed quickly by the "coiling up" to a random coil.

Figure 3B is a plot of the radius of gyration (R_g) as a function of time for the melting process shown in Figure 3A. The R_g reaches an approximately constant value after 15 ps, and the ratio of the end-to-end distance squared to the radius of gyration squared (EED^2/R_g^2) is approximately 6. From a fit to an exponential (see section II), a rate constant of 5.8×10^{-2} ps^{-1} was determined.

Figure 3C is the same type of plot as Figure 3A but for a once-folded polyethylene chain containing 207 CH_2 groups. Comparison of plots A and B of Figure 3 shows that the single extended-chain and the folded-chain molecules behave similarly in the transition process. In particular, the initial step is the movement of the ends of the chain away from their position in the crystal, followed by motion in the center and then by the coiling of the chain. The rate constant for the transition of the single, folded chain is 6.7×10^{-2} ps^{-1}. This is somewhat larger than that determined in Figure 3A, indicating that the process is faster for the folded chain. This is an interesting point since *thermodynamically* one would expect a slower rate for the more than twice as long folded chain of the same crystal length as the extended chain.[24]

To investigate the meaning of this result, we have carried out a more extensive set of calculations on the rate of transition to random coils for chains with single and multiple folds. A summary of the transition rates as a function of the number of atoms, number of folds, and temperature is given in Table II. In this table, the rate constants are, again, determined as described in section II. There are two different potentials examined in this table. The first column is without torsional potential (eq 7b); the second is for the torsional potential given by eq

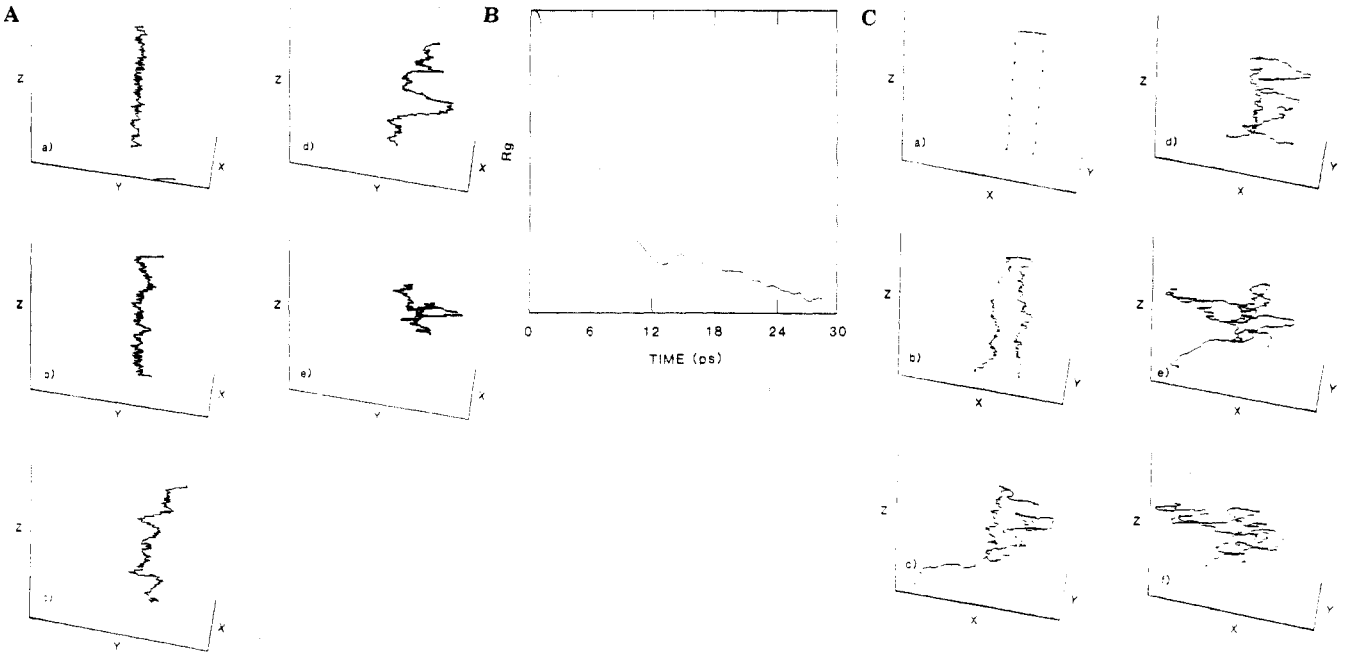

Figure 3. (A) Change of the molecular conformation of a PE extended chain (100 atoms) as a function of time on fusion at high temperature. The conformations are at 1, 6, 8, 10, and 20 ps. The temperature is 800 K; i.e., the figures represent transition at high temperature. The axes are labeled x, y, and z, which correspond to the a, b, and c axes in Figure 1, respectively. (B) Radius of gyration as a function of time for the trajectory of (A). (C) Same as for (A) except for a singly folded PE chain (207 atoms). The first conformation is at time zero.

Table II
Melting Rate for High ΔT ($\Delta T = T - T_m°$) as a Function of Molecular Length, Number of Folds, and Temperature

no. of atoms	no. of folds	rate (ps^{-1}) with 4-body potl = 0 eq 7b, T = 600 K	rate (ps^{-1}) with 4-body potl, eq 7a, T = 800 K
100	0	5.70×10^{-2}	5.80×10^{-2}
200	0	4.01×10^{-2}	4.07×10^{-2}
300	0	3.60×10^{-2}	3.90×10^{-2}
400	0	3.53×10^{-2}	3.90×10^{-2}
500	0	2.90×10^{-2}	3.30×10^{-2}
207	1	8.49×10^{-2}	6.70×10^{-2}
1007	1	1.20×10^{-1}	1.40×10^{-1}
314	2	1.04×10^{-1}	8.70×10^{-2}
421	3	1.05×10^{-1}	1.10×10^{-1}
528	4	1.28×10^{-1}	1.84×10^{-1}

no. of atoms	no. of folds	T, K	rate (ps^{-1}) with 4-body potl, eq 7a
207	1	1200	1.10×10^{-1}
314	2	1000	1.37×10^{-1}
314	2	1200	1.60×10^{-1}
421	3	1200	1.94×10^{-1}
528	4	1200	2.47×10^{-1}

7a. The temperatures are purposely high due to limitations on the computation time. An approximation to the equilibrium transition temperature was determined by finding the minimum temperature that resulted in a transition within 200 ps. The time equilibrium transition temperature would be lower than that temperature, but simulations on the nanosecond time scale would be required for its determination.

There are several important results evident from Table II. First, the effect of the torsion is to make the PE chain stiffer and thus require a higher temperature for a similar transition rate, i.e., 800 vs 600 K. Second, as in our previous study,[10] the rate decreases with increasing molecular length for extended-chain molecules (zero folds). Third, from the bottom portion of Table II, one can see that the transition rate of one to four folds per chain increases with temperature. The change of the transition rate with temperature is similar to that observed in our

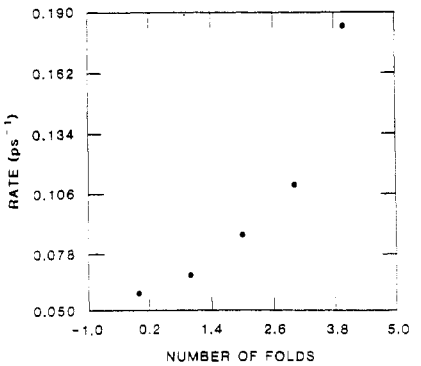

Figure 4. The high ΔT-transition rate vs the number of folds (0, 1, 2, 3, and 4) in a PE chain with a constant chain fold length of 100 atoms and increasing chain length. Each fold contains 7 atoms (i.e., the molecular lengths are 100, 207, 314, 421, and 528 atoms, respectively). The temperature is 800 K.

previous study on extended chains.[10] The main point is the effect of folding on the transition rate. It is clear from Table II that the transition rate increases as the number of folds is increased at constant fold length (i.e., with increasing molecular length). The increasing transition rate as a function of increasing folding at constant chain fold length is shown more clearly in Figure 4.

We briefly mention at this point that the transition rate is also sensitive to the bending force. If the potential is changed from eq 5 to eq 6, the melting rate for an extended chain of 100 atoms is 9.9×10^{-3} ps^{-1}, i.e., only one-sixth of that for the molecule with the more flexible bending potential (eq 5) shown in Table II. Similar results are found for the folded chains and for the onset of the condis transition of a crystal of PE discussed in an earlier publication.[4]

While the transition rate for the extended chains increases for increasing temperature, we find that for the temperatures studied in Table II, the logarithm of the rate deviates from a linear dependence on $1/T$. This same deviation was noted in our previous study. A plot of ln (rate) vs $1/T$ is linear only for temperatures that are not

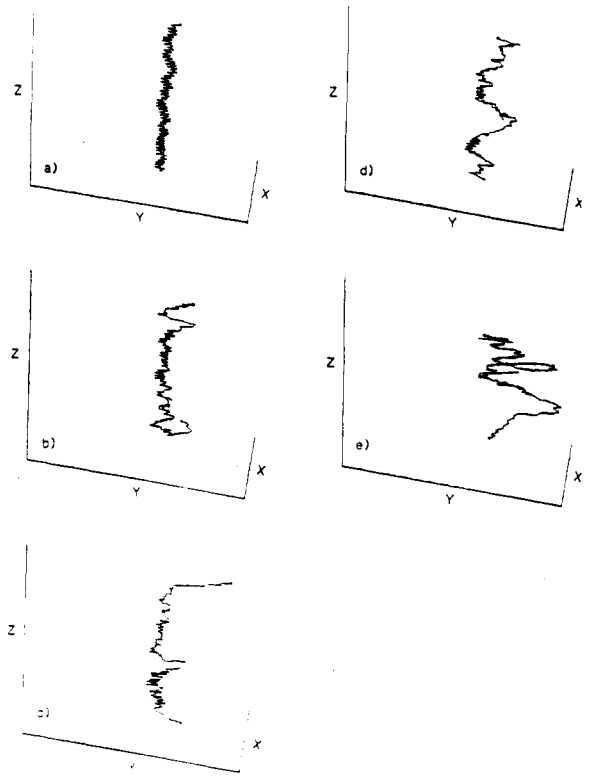

Figure 5. Change of the molecular conformation of a PE chain along a low-ΔT ($\Delta T = T - T_m°$) pathway to melting at 1, 5, 10, 20, and 25 ps. The temperature is 700 K.

in too great excess of the equilibrium melting temperature. For high temperatures there was a marked deviation from linearity (see Figure 5 to ref 10). This observation suggests that there are two melting mechanisms.

Figure 5 shows the changes in molecular conformation of an extended-chain molecule of 100 CH_2 groups for a temperature that is close to but above the equilibrium melting temperature. A comparison of Figures 5 and 3A shows that there are two different transition mechanisms. The principal difference is the longer time required for diffusion of the center of the chain for low ΔT. The initial step is again the movement of the ends of the chain. This is followed by the formation of loops that change in size until the middle of the chain begins to move, which is then followed by the coiling.

To elucidate the different melting mechanisms at low ΔT, we have plotted the average position 10-atom segments above the crystal surface. Figure 6A is the plot of the 10-atom segment at the end of the chain vs time. This figure corresponds to the motion shown in Figure 5. The motion away from the surface is initially very rapid (initial 4 ps). The loop then appears to find new lattice sites on the crystal surface and lies back into a stable orientation with most atoms on the surface. This is a crystallization process. Crystallization of the chain is thus a competing process with melting (melting rate $\simeq$ crystallization rate). This competition between melting and crystallization continues until the middle of the chain begins to move at $\simeq$14 ps. Figure 6B illustrates the motion of the center segment of 10 atoms relative to the crystal surface. At about 14 ps, the center segment starts significant motion. At this time the rate of melting becomes larger and dominates the overall process.

The low-ΔT melting/crystallization process can be seen even more clearly in Figure 7. In Figure 7A, a situation has been simulated in which there is a crystalline segment (60 atoms) and an amorphous segment (40 atoms) of the

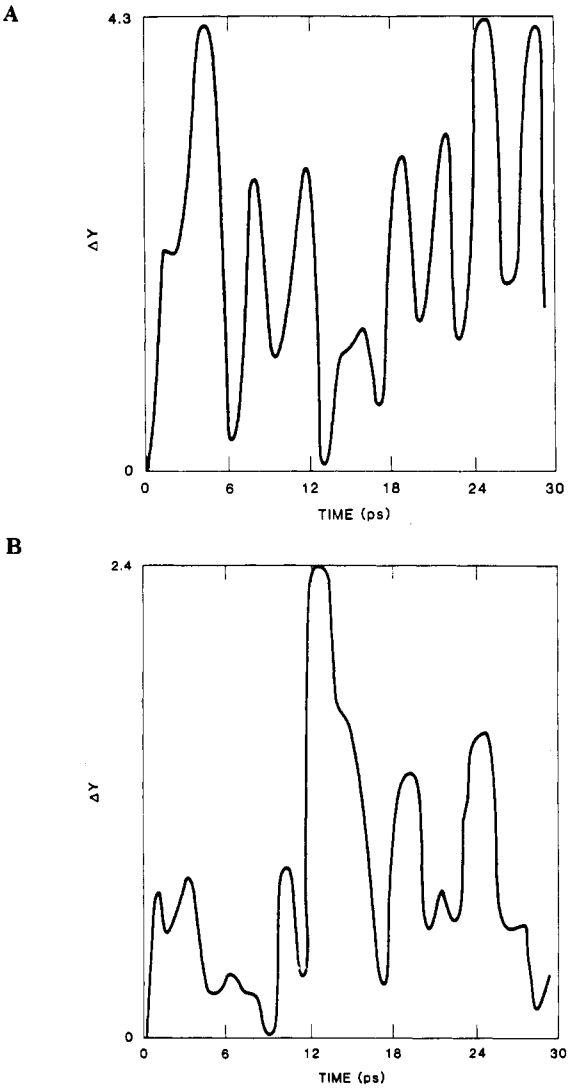

Figure 6. (A) Average elevation of a 10-atom segment above the crystal surface at the end of the PE chain of Figure 5 as a function of time. (B) Same as for (A), except for a 10-atom segment in the center of the PE chain.

100-atom PE chain. Continuing with the simulation for 5 ps leads to a conformation within which the amorphous segment crystallizes (Figure 7B) along lattice sites of the adjacent crystal cell. The atoms assume again a planar trans conformation. The molecule has at this moment crystalline regions that are joined by a short amorphous segment. Work is in progress to elucidate this crystallization process further.

In contrast to the low-ΔT mechanism, the high-ΔT mechanism appears to largely bypass the competing crystallization. Figure 8 shows the average elevation above the crystal surface for a 10-atom segment located at the end (Figure 8A) and the center (Figure 8B) of the chain for the high-ΔT process. The center segment begins to move already at very short times of $\simeq$5 ps (Figure 8B).

Table III and Figure 9 give a summary of the results for the low-ΔT melting rates. Comparisons of Figures 4 and 9 and Tables I and III show that there are two different mechanisms for the transition. The low-ΔT process matches the experimental results on melting[23,24] more closely. That is, the rate of melting decreases with increasing number of folds, and for a single, extended chain, the rate is linear as a function of $1/T$.

B. Diffusion of Segments. The melting of equilibrium crystals starts from the upper and lower edges of

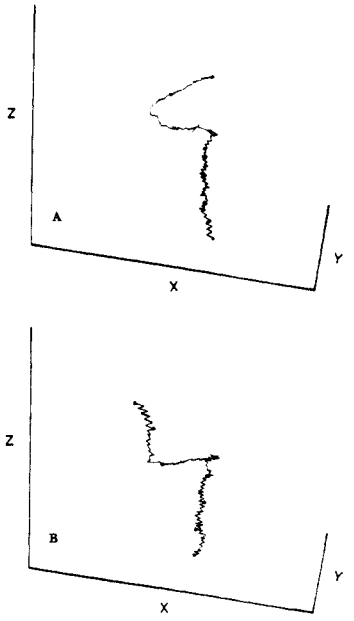

Figure 7. (A) Conformation of a 100-atom PE chain with a 60-atom crystalline region and a 40-atom amorphous region. (B) Same as for (A), except after 5 ps of time.

the outer, lateral crystal surfaces and proceeds by peeling off layer after layer of molecular chains in a direction perpendicular to the crystal surface.[10] This process has been demonstrated in part A of this section and is observed experimentally. The melting of a single chain starts at a chain end or fold at the edge of the crystal, continuing down the lateral surface. Thus, the rate of diffusion of the chain ends should be greater than that for the center of the chain. Table IV shows the diffusion coefficients for various 10-atom segments of a 100-atom extended polyethylene chain on a crystal surface and that for a singly folded chain of 207 CH_2 groups. The diffusion coefficients were calculated as described in section II. From Table IV, it can be seen that the diffusion of the end 10 atoms of a PE chain is faster than that for the 10-atom segment 30–39 or the middle segment 46–54. The fastest diffusion is found for the atoms in the fold. This seems to happen because the folds are in a "metastable" state and rapidly rearrange in order to find a more stable geometry. The effect of increasing temperature is to increase the diffusion coefficients.

IV. Conclusions

The transition to the random coil is strongly dependent on temperature and number of folds in a chain. Besides nonbonded forces, hindered rotation and bending modes have the greatest influence on the melting rate. Making the chain less flexible reduces the melting rate. The diffusion coefficients provide evidence that the transition occurs by peeling off the chain from the crystal surface from the ends or the folds. These conclusions are in excellent agreement with our previous experimental[25] and theoretical studies.[10,16]

The temperature dependence of the transition process for folded chains was found to be more complex than that for extended chains. While the above conclusions on the initial steps to melting still remain unchanged, there are two distinctly different overall mechanisms for the transition process. For temperatures with low ΔT, the process follows the expected trend of decreasing transition rate with increasing number of folds at a constant lamellar thickness. This pathway from the crystalline state to the liquid phase involves a competition between melting

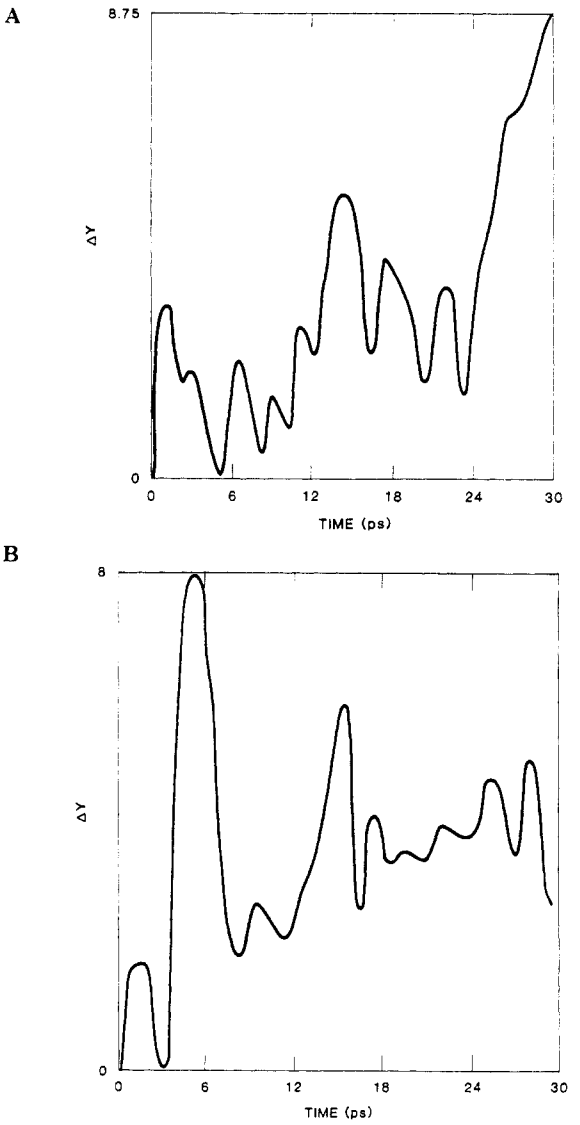

Figure 8. (A) Same as for Figure 6A, except for the high-ΔT melting pathway. (B) Same as for Figure 6A, except for a 10-atom segment in the center of the PE chain.

Table III
Melting Rate for Low ΔT ($\Delta T = T - T_m^\circ$) as a Function of Molecular Length and Number of Folds

no. of atoms	no. of folds	rat (ps^{-1}) with 4-body potl = 0, eq 7b, T = 500 K	rate (ps^{-1}) with 4-body potl, eq 7a, T = 700 K
100	0	4.0×10^{-2}	4.1×10^{-2}
200	0	2.5×10^{-2}	3.4×10^{-2}
300	0	2.1×10^{-2}	3.2×10^{-2}
400	0	1.7×10^{-2}	2.7×10^{-2}
500	0	1.4×10^{-2}	2.1×10^{-2}
207	1	3.1×10^{-2}	3.7×10^{-2}
314	2	2.7×10^{-2}	3.5×10^{-2}
421	3	2.5×10^{-2}	2.8×10^{-2}
528	4	2.0×10^{-2}	2.3×10^{-2}

and crystallization. The competition between melting and crystallization continues until the center of the chain begins to diffuse. At this time, the process is shifted toward melting and the polymer chain reaches quickly a randomly disordered geometry (random coil).

For temperatures with a $\Delta T \geq 100$ K, the melting process is different. In this case the total energy available is sufficient to cause a rapid propagation of the "peeling-off process" to the center of the polymer chain. While the initial events are similar to the first mechanism, the time required to increase the melting/crystallization rate ratio

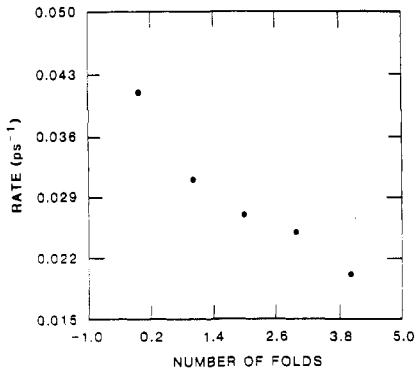

Figure 9. Low-ΔT melting rate vs the number of folds in a PE chain with a constant length of 100 atoms between folds. Each fold contains 7 atoms. The temperature is 700 K.

Table IV
Segment Diffusion Coefficients for a Polyethylene Chain (100 Atoms) on a Polyethylene Surface

D, cm^2/s	segment of PE	temp, K
4.2×10^{-4}	1–10	400
4.6×10^{-4}	1–10	600
4.1×10^{-4}	30–39	400
4.3×10^{-4}	30–39	600
3.5×10^{-4}	46–55	400
3.7×10^{-4}	46055	600
	207 Atoms and 1 Fold	
4.1×10^{-4}	1–10	400
3.4×10^{-4}	30–39	400
2.9×10^{-4}	46–55	400
4.7×10^{-4}	fold	400
4.4×10^{-4}	1–10	600
4.3×10^{-4}	30–39	600
4.3×10^{-4}	46–55	600
4.8×10^{-4}	fold	600

is much shorter. In short, the polymer chain goes practically directly to the melt, bypassing much of the competing crystallization. For extended chains, the temperature dependence of either mechanism is qualitatively the same. For folded polymers, the added instability of the folds leads to a greater shift in the melting/crystallization rates and leads to a kinetic effect of increasing the rate for melting with increasing folding.

The observed fact that there are two different melting mechanisms is interesting in light of recent studies on crystal melting of metals. Phillips et al.[27] have recently described observations from molecular dynamics simulations of the melting process of silicon. They concluded that there are two different processes, one that they call thermodynamic melting and one they call mechanical melting. These results on silicon are in good agreement with our simulations on polyethylene.

Acknowledgment. This research was sponsored by the Division of Materials Science, Office of Basic Energy Science, U.S. Department of Energy, under Contract DE-AC05-84OR21400 with Martin Marietta Energy Systems, Inc., and the Materials Division of the National Science Foundation, Polymers Program, under Grant DMR8818412. Some of the calculations reported here were carried out on the Cray X-MP/48, Grant TRA-890046N, Projects YPO, XCK, National Center for Supercomputing Applications (NCSA), at the University of Illinois at Urbana–Champaign. Other calculations were performed on the IBM 3090 at The University of Tennessee (UTCC).

References and Notes

(1) Wunderlich, B.; Melillo, L.; Cormier, C. M.; Davidson, T.; Snyder, G. *J. Macromol. Sci.* **1967**, *B1*, 485.
(2) Czornyj, G.; Wunderlich, B. *J. Polym. Sci., Polym. Phys. Ed.* **1977**, *15*, 1905.
(3) Wunderlich, B. *Faraday Discuss. Chem. Soc.* **1979**, *68*, 237.
(4) Noid, D. W.; Sumpter, B. G.; Varma-Nair, M.; Wunderlich, B. *Makromol. Chem., Rapid Commun.* **1989**, *10*, 367; *Macromolecules* **1990**, *23*, 664.
(5) Wunderlich, B.; Grebowicz, J. *Adv. Polym. Sci.* **1984**, *60/61*, 1. Wunderlich, B.; Möller,M.; Grebowicz, J.; Baur, H. *Adv. Polym. Sci.* **1988**, *87*, 1.
(6) Shu, P. H.-C.; Wunderlich, B. *J. Cryst. Growth* **1980**, *48*, 227.
(7) Crystal, A. H. *J. Polym. Sci., Polym. Phys. Ed.* **1970**, *8*, 2153.
(8) Kovacs, A. J.; Gonthier, A.; Straupe, C. *J. Polym. Sci., Polym. Symp.* **1975**, *No. 50*, 283.
(9) Kovacs, a. J.; Straupe, C.; Gonthier, A. *J. Polym. Sci., Polym. Symp.* **1977**, *No. 59*, 31.
(10) Noid, D. W.; Pfeffer, G. A.; Cheng, S. Z. D.; Wunderlich, B. *Macromolecules* **1988**, *21*, 3482.
(11) Mehta, A.; Wunderlich, B. *J. Polym. Sci., Polym. Phys. Ed.* **1974**, *12*, 255.
(12) Wunderlich, B.; Mehta, A. *Colloid Polym. Sci.* **1975**, *25*, 193.
(13) Cheng, S. Z. D.; Wunderlich, B. *J. Polym. Sci., Polym. Phys. Ed.* **1986**, *24*, 577.
(14) Cheng, S. Z. D.; Wunderlich, B. *J. Polym. Sci., Polym. Phys. Ed.* **1986**, *24*, 595.
(15) Cheng, S. Z. D.; Bu, H.-S.; Wunderlich, B. *J. Polym. Sci., Polym. Phys. Ed.* **1988**, *26*, 1947.
(16) Cheng, S. Z. D.; Noid, D. W.; Wunderlich, B. *J. Polym. Sci., Polym. Phys. Ed.* **1989**, *27*, 149.
(17) Flory, P. J. *Proc. R. Soc. London, Ser. A* **1956**, *234*, 60.
(18) Gujrati, P. D.; Goldstein, M. *J. Chem. Phys.* **1980**, *74*, 2596. Gujrati, P. D. *J. Phys. A: Math. Gen.* **1980**, *13*, 2437. Gujrati, P. D. *J. Stat. Phys.* **1982**, *28*, 441.
(19) Goldstein, M. *Classical Mechanics*; Addison-Wesley: Reading, MA, 1950; Chapter 7.
(20) Shampine, L. F.; Gordon, M. K. *Computer Solution of Ordinary Differential Equations: The Initial Value Problem*; Freeman: San Francisco, 1975.
(21) Noid, D. W.; Sumpter, B. G.; Wunderlich, B.; Pfeffer, G. A. *J. Comput. Chem.* **1990**, *11*, 236.
(22) Allen, M. P.; Tildesley, D. J. *Computer* Simulation *of Liquids*; Oxford University Press; Oxford, 1987.
(23) Essen, H. *OCPE Bull.* **1983**, *3*, 13, Program 452.
(24) Wunderlich, B. *Macromolecular Physics. Crystal Melting*, Vol. 3.
(25) Cheng, S. Z. D.; Zhang, A.; Chen, J.; Heberer, D. P. *J. Polym. Sci., Polym. Phys. Ed.*, in press.
(26) Prime, R. B.; Wunderlich, B.; Melillo, L. *J. Polym. Sci., Polym. Phys. Ed.* **1969**, *7*, 2091.
(27) Phillips, S. R.; Yip, S.; Wolf, D. *Comput. Phys.* Nov/Dec 1989, 20.